Chevalier, M., et al., 2020, Temperature change in subtropical southeastern Africa during the past 790,000 yr: Geology, v. 49, https://doi.org/10.1130/G47841.1

Appendix S1: Selection of pollen taxa used for the reconstruction

In this study, we followed the standard procedure to reconstruct climate from fossil pollen (Birks et al., 2010). We excluded pollen types of aquatic plants (15 taxa) from the sum before calculating the percentages. We then excluded all the pollen taxa that represent large families or tribes (9 taxa), because the diversity of the climate response of so many composing species is too large to produce informative *pdfs* (*e.g.* Poaceae is composed of 547 species across the selected calibration zone, Supplemental Figure S1). Some taxa were absent from our study area (*e.g. Persicaria senegalensis*-type) or in insufficient quantities to infer robust *pdfs* (less than 25 presence records, *e.g. Elaeis guineensis*) and could not be included (12 and 23 taxa, respectively). We also excluded Aizoaceae and Chenopodiaceae/Amaranthaceae, as species from these groups preferentially respond to non-temperature variables. We did not apply any minimum percentage filtering. In total, we retained 166 from the original total of 216 terrestrial taxa (Supplemental Table S1). On average, we used 18 taxa per sample to reconstruct MAT (minimum 5 – maximum 38). Collectively, these taxa represent 67% of the terrestrial pollen taxa (minimum 43% - maximum 93%)

The density of data points varies across the study area, with South Africa and East Africa providing most of the data. However, sufficient information is available between these two regions to estimate reliable climate responses (see Fig. 2C in the main text). The selected taxa cover a large range of MAT conditions and the minimum and maximum 'reconstructible' MAT values (optima of the coldest and warmest taxa, 11.9 and 26.3°C) are much colder and warmer than the coldest and warmest reconstructed MAT values (16.4 and 21.6°C, respectively; Supplemental Figure S2). This suggests that the full range of temperature variability reconstructed is not limited by the calibration dataset.

Table S1: Summary of all the selected and excluded terrestrial pollen taxa observed in the record based on their availability in the GBIF (Global Biodiversity Facility Database) (GBIF.org, 2018e, 2018i, 2018f, 2018a, 2018d, 2018h, 2018g, 2018c, 2018b) for CREST dataset version 5 (Chevalier, 2018) and their sensitivity to Mean Annual Temperature across the study area.

Excluded taxa	Undetermined taxa	Indeterminata, Stephanocolporate, striatoreticulate, Varia
	Aquatic taxa and spores	Riccia-type, Anemia-type, Anthoceros, Phaeoceros, Lycopodium, Lycopodium cernuum-type, Polypodiaceae, Pteridium-type, Pteris, Cyperaceae, Nymphaea, Typha, Monolete psilate, Spores monolete, Spores trilete
	Large families or tribes	Asteraceae Liguliflorae, Asteraceae Tubuliflorae, Asteraceae Vernoniae, Caesalpiniaceae, Daisy-type, Fabaceae undiff., Mimosoideae, Poaceae undiff., Rubiaceae undiff.
	Insensitive taxa	Aizoaceae, Chenopodiaceae/Amaranthaceae
	Absent from the calibration area	*Afraegle*, *Buxus*, *Buxus madagascaria*-type, *Daniellia*-type, *Detarium*, *Dichostemma-Anthostema*-type, *Klaineanthus*, *Lophira*, *Notobuxus*, *Nypa*, *Persicaria senegalensis*-type, *Stipularia africana*
	Insufficient data points	*Allanblackia*, *Berlinia*-type, *Borassus*, *Calamus*, *Canarium*, *Caperonia*-type, *Casuarina*, *Cephalosphaera*, *Cuviera*, *Cynometra*, *Elaeis guineensis*, *Flabellaria*, *Gaertnera*, *Garcinia ovalifolia*-type, *Heritiera*-type, *Leea*, Liliaceae, *Luffa*, *Lumnitzera*-type, *Mitracarpus*, *Pandanus*, *Pycnanthus*, *Raphia*-type
Selected taxa		*Acalypha*, Acanthaceae undiff., *Adenia*, *Afzelia*, *Alchemilla*, *Alchornea*, *Allophylus*, *Aloe*-type, *Ammannia*, *Anthocleista*, *Anthospermum*-type, *Avicennia*, *Balanites*, *Baphia*-type, *Barringtonia*, *Basella*, *Bauhinia*, *Blighia*-type, *Boscia*/*Maerua*-type, *Brachystegia*, Brassicaceae, *Bridelia*, *Burkea*, Campanulaceae undiff., *Canthium*/*Morelia*-type, *Capparis*, Caryophyllaceae undiff., *Cassia*-type, Celastraceae, *Celtis*, *Centaurea*, *Chrysophyllum*, *Cissus*, *Clematis*-type, *Cleome*, *Cliffortia*, *Clutia*, *Cnestis*-type, *Coccinia*, *Coffea*-type, *Colophospermum mopane*, Combretaceae-type, Commelinaceae, *Commiphora*, *Corchorus*, *Cordia*, *Cotula*-type, *Crossopteryx*-type, *Crotalaria*, *Croton*, *Cucumis*, *Cussonia*, *Dialium*, *Diospyros*, *Dodonaea viscosa*, *Dombeya*, *Dracaena*, *Drosera*, Ericaceae, *Eriocaulon*, *Erythrina*, *Euclea*, *Eugenia*, *Euphorbia*, *Fagonia*, *Flagellaria*, *Flueggea*, *Galium*, *Gazania*-type, *Grewia*, *Gunnera*, *Hagenia*, *Hermannia*, *Hymenocardia*, Hyphaene, *Hypoestes*/*Dicliptera*-type, *Ilex*, *Impatiens*, *Indigofera*-type, *Ipomoea*, *Juniperus*, *Justicia*/*Blepharis*-type, *Khaya*, *Kigelia africana*, *Kohautia*, *Lannea*-type, *Leonotis*, *Lobelia*, *Ludwigia*, *Macaranga*, *Manilkara*, *Markhamia*, *Melochia*, *Merremia-Hildebrandtia*-type, *Millettia*, *Mitragyna*, *Moraceae*, *Morella*, *Myriophyllum*, *Myrsine africana*, Neuradaceae, Nyctaginaceae, *Ocimum*-type, *Olea*, *Ormocarpum*, *Oxygonum*, *Parinari*, *Passerina*, *Pelargonium*-type, *Peltophorum africanum*, *Pentzia*-type, *Pericopsis*, *Petalidium*, *Philenoptera*/*Lonchocarpus*-type, *Phoenix*, *Phyllanthus*, *Piptadeniastrum*/*Entada*-type, *Plantago*, *Plicosepalus*, *Podocarpus*, *Polycarpaea*, *Polycarpon*, *Polygala*, *Polygonum aviculare*-type, *Protea*-type, *Pseudolachnostylis*-type, *Psychotria*, *Psydrax*, *Pterocarpus*-type, *Rauvolfia*, Restionaceae, Rhamnaceae undiff., Rhizophoraceae, *Rhynchosia*, *Rumex*, *Rytigynia*/*Fadogia*-type, Sapotaceae/Meliaceae, *Scabiosa*/*Cephalaria*-type, *Schefflera*, *Schrebera*-type, Scrophulariaceae undiff., *Searsia*, *Seddera*/*Evolvulus*-type, *Solanum*, *Sorindeia*, *Spermacoce*, *Spirostachys africana*, *Sterculia*, *Stereospermum*, *Stoebe*-type, *Strophanthus*, *Strychnos*, *Tamarindus*, *Tapinanthus*, *Tarchonanthus*/*Artemisia*-type, *Tephrosia*-type, Thymelaeaceae undiff., *Tribulus*, *Uapaca*, Urticaceae, *Vachellia*/*Senegalia*, *Vigna*, *Waltheria*, *Zanthoxylum*, *Ziziphus*-type, *Zygophyllum*

Temperature v. precipitation reconstructions:

We focused on reconstructing MAT because previous studies have shown the presence of a strong temperature component in the pollen data (Dupont et al., 2011, 2019). MAT being fairly homogeneous, making the reconstruction from the regionally-averaged pollen data can lead an accurate estimate of past temperature variability in the region. In contrast, while CREST has been shown to be able to produce reliable quantified precipitation estimates from discrete sites (Chevalier and Chase, 2015), many local and regional factors can define precipitation, rendering it vastly more complex to properly simulate at the spatiotemporal resolution of the record. Qualitative assessments of past environmental change across the catchment are reasonable, but precise quantitative estimates of precipitation (*e.g.* 400 mm of rainfall), as produced by CREST, are much more demanding. Considering this, we determined that the nature of the MD96-2048 catchment precludes the quantitative reconstruction of distinct climatic parameters related to the hydrologic cycle.

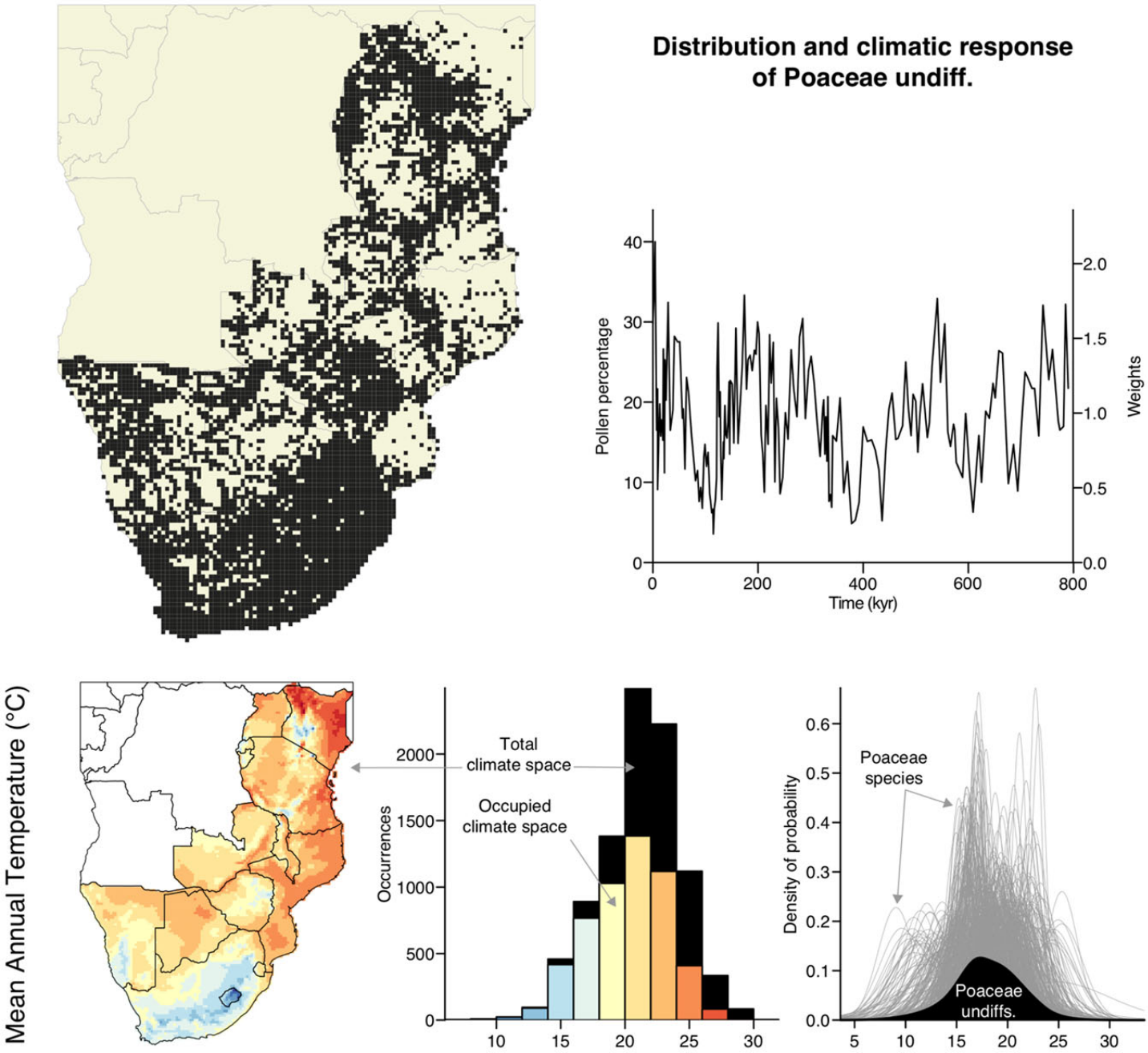

Figure S1: Summary diagram of the distribution (top) and climatic response (bottom) of 'Poaceae undiff.' across the study area. The diversity of Poaceae species is so high (547 species) that every part of the climate space is colonised by one or more species (black grid cells on the map). This diagram was automatically generated by the CREST software v4.1.1 (Chevalier et al., 2014) and derived from the GBIF for CREST calibration dataset v5 (Chevalier, 2018).

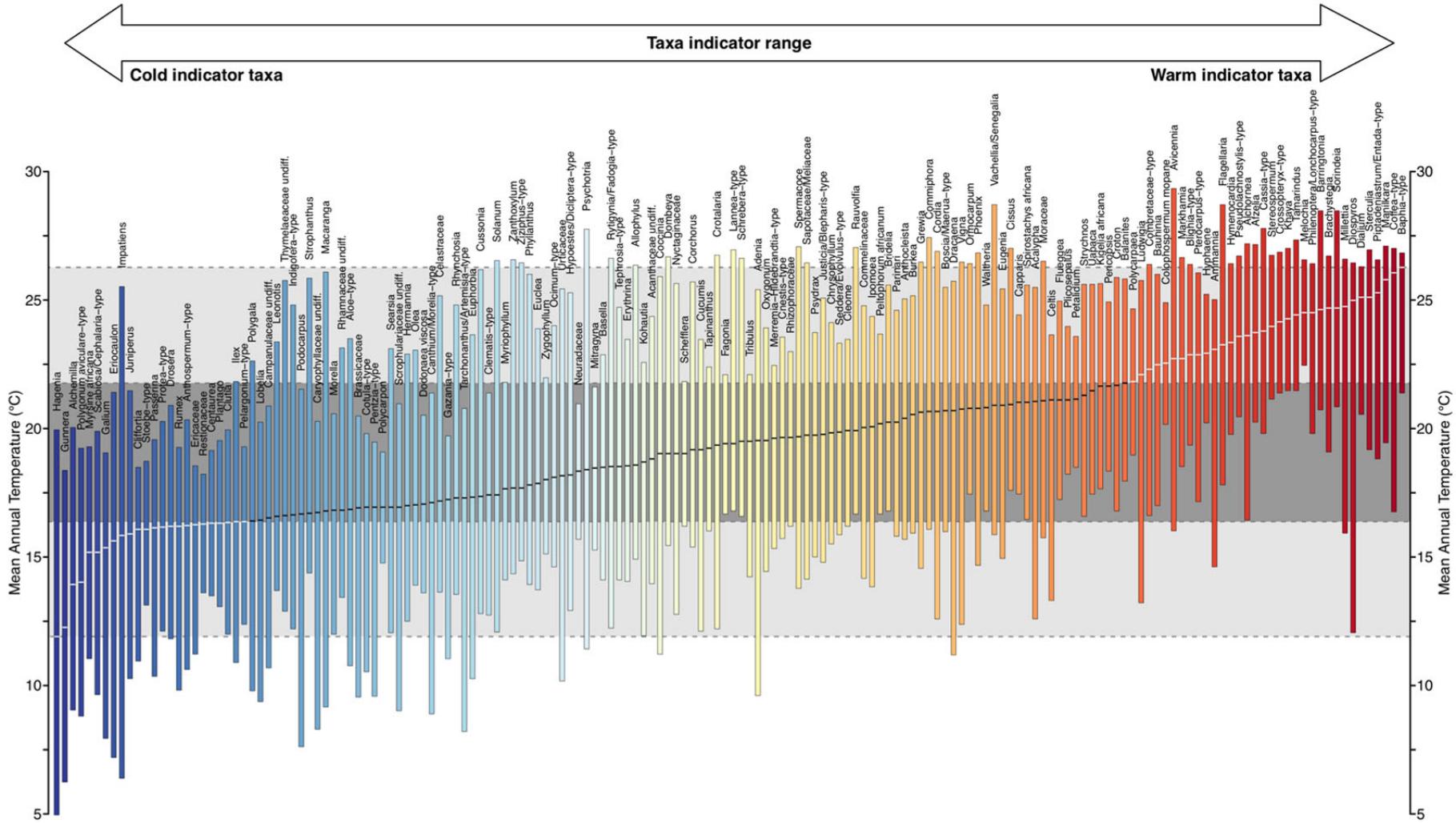

Figure S2: Simplified representation of the *pdfs* (95% range; coloured rectangles) of the 166 taxa selected to reconstruct MAT and sorted from left to right by their climate optimum (black or white bar in the coloured rectangles). The light grey rectangle in the background represents the range of 'reconstructible' MAT values (defined by the minimum and maximum optima of the coldest and warmest taxa, respectively) and the dark grey rectangle the reconstructed range.

Appendix S2: Comparison of MAT with independent regional and global temperature records

We compared our MAT reconstructions with the few other long records that exist in Africa, as well as global indicators of past temperature variability (Supplemental Figure S3). These comparisons highlight a strong coherence of temperature variability globally (Supplemental Table S2). To allow comparisons between records, we interpolated all records at a 1-kyr resolution using a Gaussian kernel smoothing approach with a kernel width defined by the mean sampling resolution of the pollen record (Δt=4.39kyrs) (Rehfeld et al., 2011). Gaussian smoothing ensures that the resolution of the interpolated records matches the resolution of the pollen record. All analyses were carried out using the R software version 3.5.2 (R Core Team, 2018).

Table S2: Cross-correlation results of the local and global temperature records discussed in this study. All correlation tests are significant with $p_{values} < 10^{-10}$ (***).

	MAT (this study)	MD96-2048 leaf wax long chain n-alkanes $C_{31} / (C_{29} + C_{31})$)	MD96-2048 sea-surface temperatures	Lake Malawi surface temperature	Global temperature (Dome C, Antarctica)	Global CO2 (Dome C, Antarctica)	Global ice (benthic $\delta^{18}O$ stack)
MD96-2048 leaf wax long chain n-alkanes $C_{31} / (C_{29} + C_{31})$)	-0.71 ***						
MD96-2048 sea-surface temperatures	0.72 ***	-0.57 ***					
Lake Malawi surface temperature	0.30 ***	-0.24 ***	0.45 ***				
Global temperature (Dome C, Antarctica)	0.72 ***	-0.66 ***	0.70 ***	0.39 ***			
Global CO2 (Dome C, Antarctica)	0.74 ***	-0.71 ***	0.72 ***	0.41 ***	0.92 ***		
Global ice (benthic $\delta^{18}O$ stack)	-0.66 ***	0.61 ***	-0.57 ***	-0.46 ***	-0.87 ***	-0.83 ***	

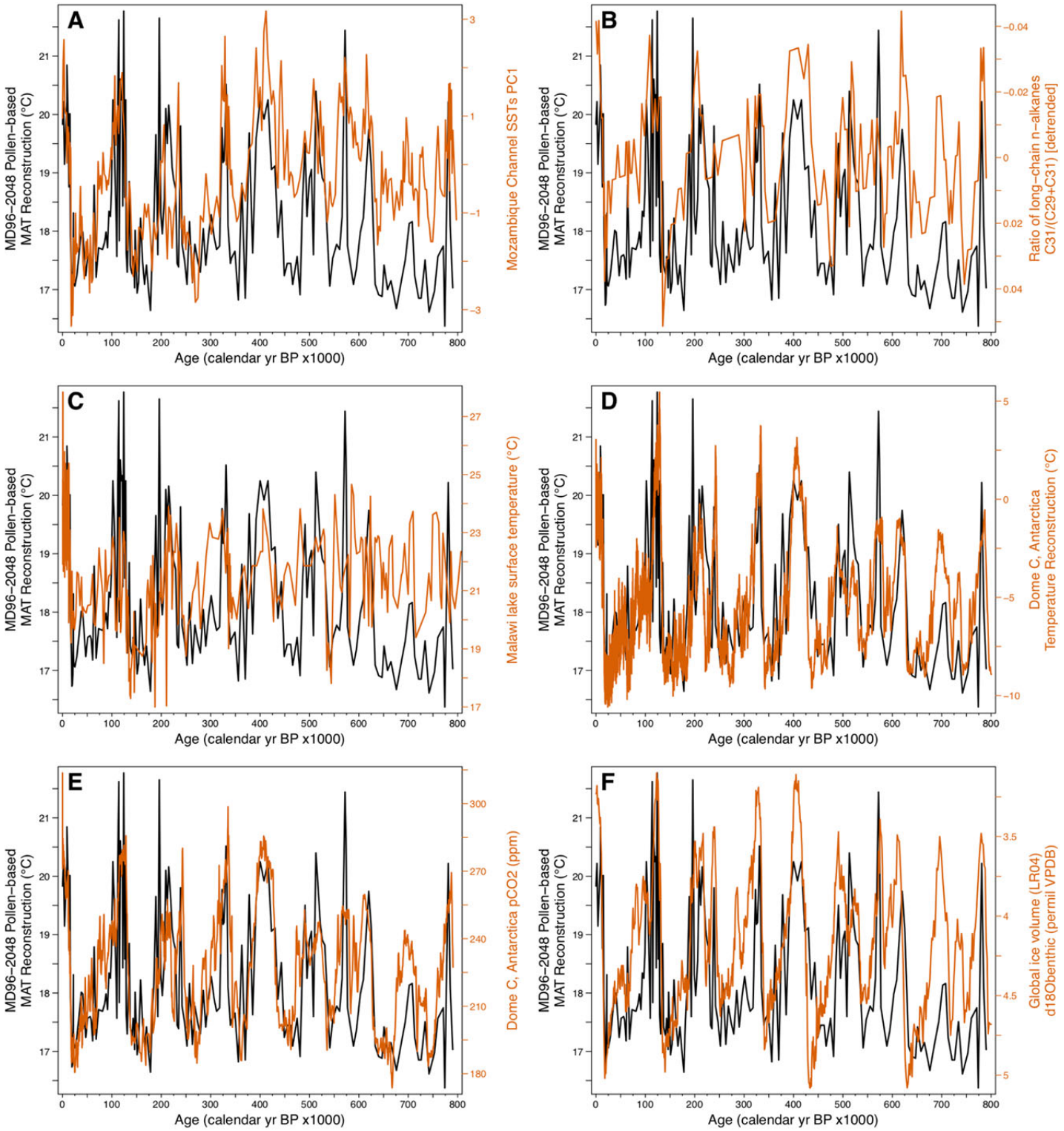

Figure S3: Comparison of our MAT reconstruction (Chevalier et al., 2020) in black with different regional (A-C) and global (D-F) temperature indicators in orange. (A) MD96-2048 Sea surface temperatures (Caley et al., 2018), (B) MD96-2048 ratio of leaf wax long chain n-alkanes C31/(C29+C31) (Castañeda et al., 2016a, 2016b), (C) Lake Malawi lake surface temperature (Johnson et al., 2016), (D) Dome C, Antarctica temperature reconstruction (Jouzel and Masson-Delmotte, 2007; Jouzel et al., 2007), (E) Dome C, Antarctica atmospheric CO2 concentration (Bereiter et al., 2015) and (F) $\delta^{18}O$ benthic stack as a proxy for global ice volume (Lisiecki and Raymo, 2005a, 2005b).

Appendix S3: Comparison of pollen diversity with independent regional and global temperature records

To identify possible effects of temperature, and glacial interglacial cycles more generally on the vegetation in the Limpopo catchment we used 6 different indices that describe diversity (Hill, 1973; Legendre and Legendre, 2012). Of the six indices presented here, only two of them incorporate the number of counts to calculate diversity: the Margalef's index and the rarefraction analysis. None of the different indices show any strong relationship with the reconstructed MAT, suggesting that there is no direct and linear relationship between pollen diversity and temperature across the Limpopo basin (Supplementary figure DR4).

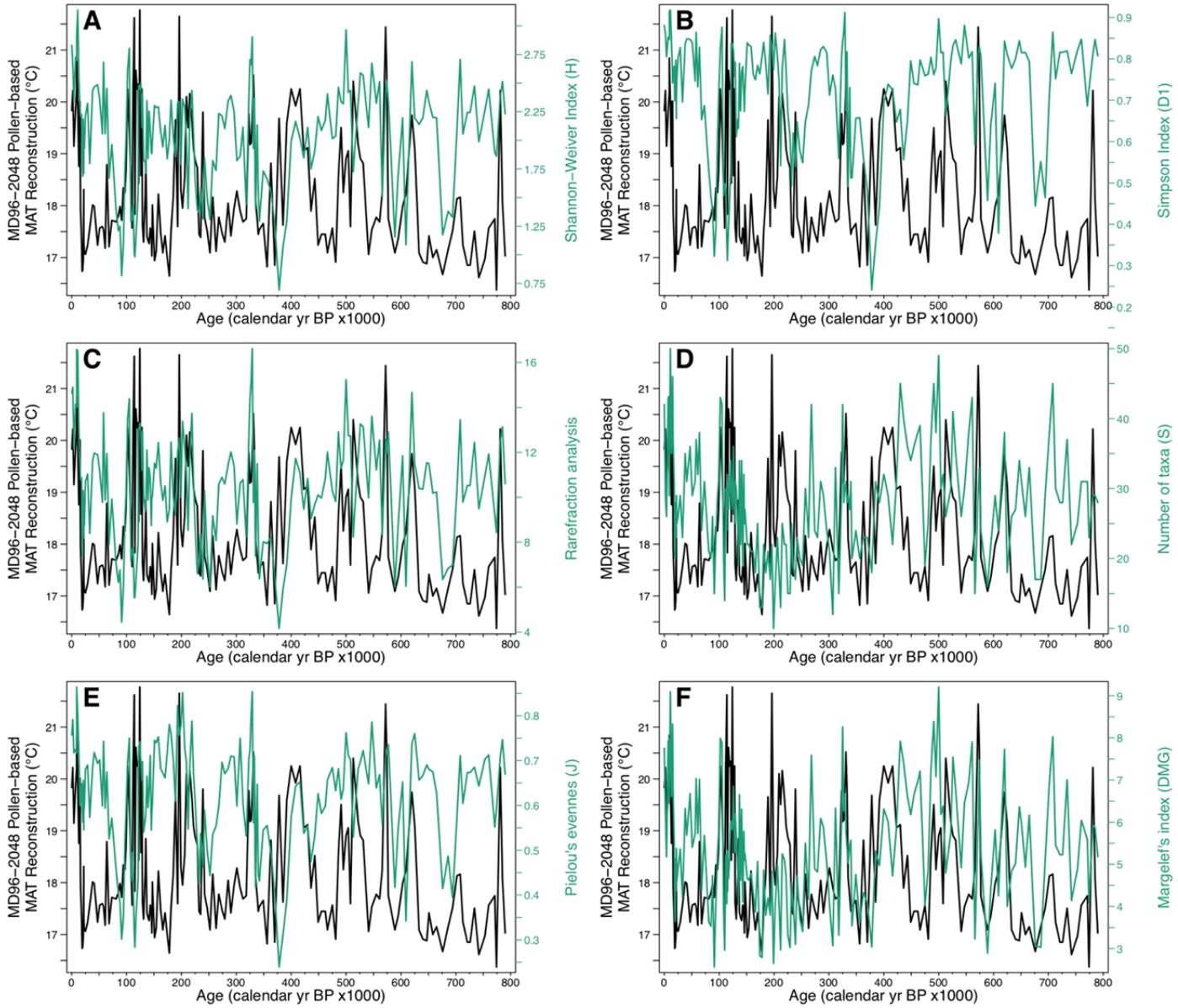

Figure S4: Comparison of our MAT reconstruction (Chevalier et al., 2020) with different measures of pollen diversity: (A) Shannon-Weiver index (Hill, 1973), (B) Simpson index (Hill, 1973), (C) Fischer's alpha (Fisher et al., 1943), (D) the number of taxa, (E) Pielou's evenness index (Pielou, 1966) and (F) Margalef's index (Margalef, 1957).

We further simplified the temperature data into categorical variables ('glacials' and 'interglacials') to assess the potential effect of these mean climate states without accounting for the actual temperature values (Supplemental Figure S5). Here, glacials and interglacials are defined by the LR04 chronology and the ages of the pollen samples. Again, we were not able to show any significant difference between pollen diversity during glacial and interglacial periods. The only result is that the spread of the diversity of interglacial periods is generally wider (larger span of the boxplots) for all the indices.

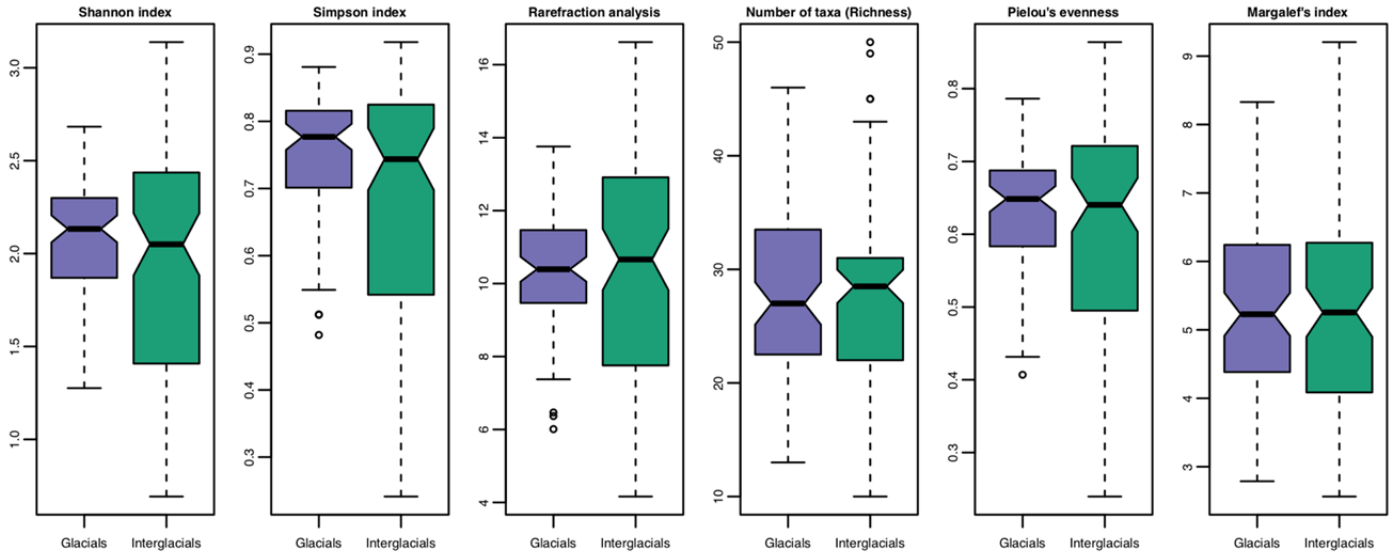

Figure S5: Spread of the different pollen diversity indices for all the glacial (purple) and interglacial (green) periods. The difference between glacials and interglacials is not significant for the six indices considered here.

The main frequencies of variability of the Margalef's index across the record (Supplemental Figure S6) differ from those of our reconstructed MAT trends (Fig. 3 in the article), further supporting the decoupling of the variability of temperature and pollen diversity. The negative influence of the 400-kyr (strong influence) and 100-kyr (weaker influence and more variable) eccentricity cycles on pollen diversity are evident.

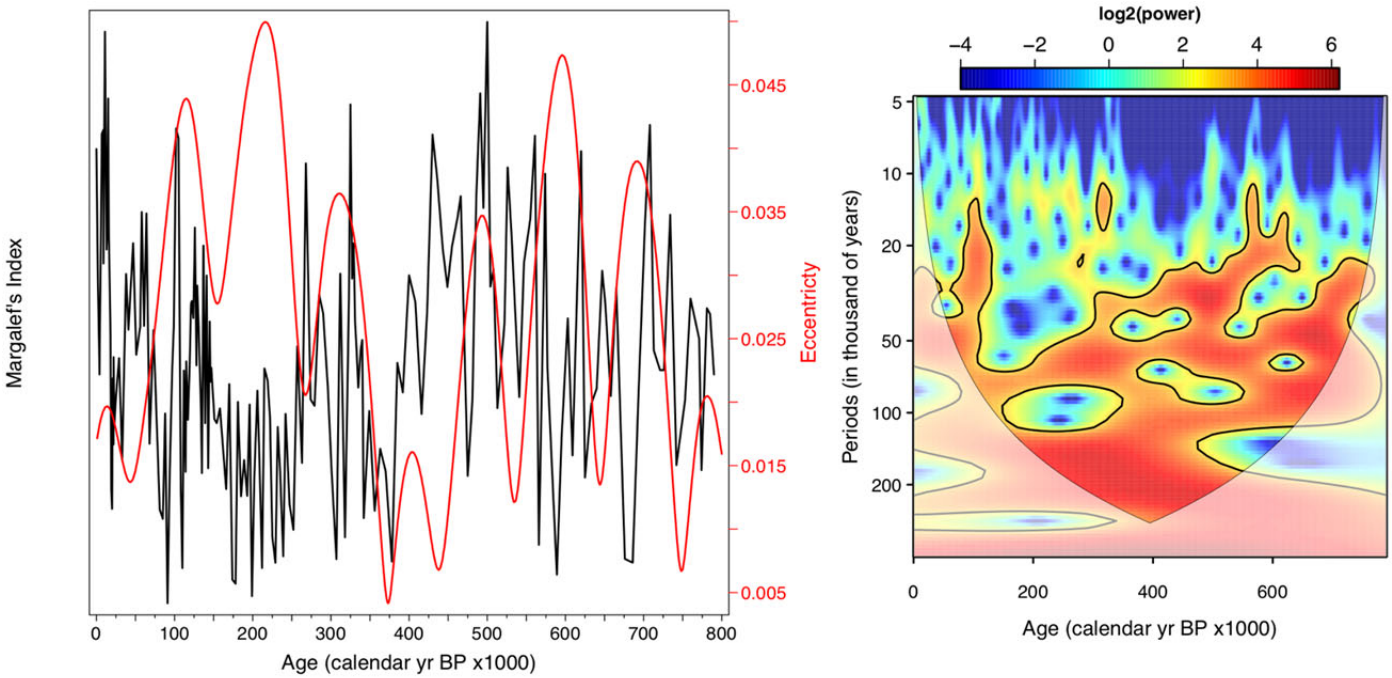

Figure S6: Comparison of the Margalef's index with eccentricity (Laskar et al., 2004). Continuous Morlet wavelet transform of Margaef's index. The panel shows the local wavelet power spectrum of the record, with black lines indicating the cone of influence to show where boundary effects are present and the regions of greater than 99% confidence using a white-noise model.

REFERENCES CITED

Bereiter, B., Eggleston, S., Schmitt, J., Nehrbass-Ahles, C., Stocker, T.F., Fischer, H., Kipfstuhl, S., and Chappellaz, J., 2015, Revision of the EPICA Dome C CO 2 record from 800 to 600 kyr before present: Geophysical Research Letters, v. 42, p. 542–549, doi:10.1002/2014GL061957.

Birks, H.J.B., Heiri, O., Seppä, H., and Bjune, A.E., 2010, Strengths and weaknesses of quantitative climate reconstructions based on Late-Quaternary biological proxies: The Open Ecology Journal, v. 3, p. 68–110, http://benthamscience.com/open/toecolj/articles/V003/S10001TOECOLJ/68TOECOLJ.pdf (accessed May 2012).

Caley, T. et al., 2018, A two-million-year-long hydroclimatic context for hominin evolution in southeastern Africa: Nature, v. 560, p. 76–79, doi:10.1038/s41586-018-0309-6.

Castañeda, I.S., Caley, T., Dupont, L.M., Kim, J.-H., Malaizé, B., and Schouten, S., 2016a, Middle to Late Pleistocene vegetation and climate change in subtropical southern East Africa: Earth and Planetary Science Letters, v. 450, p. 306–316, doi:10.1016/j.epsl.2016.06.049.

Castañeda, I.S., Caley, T., Dupont, L.M., Kim, J.-H., Malaizé, B., and Schouten, S., 2016b, Plant leaf wax (n-alkane) data from sediment core MD96-2048:, doi:10.1594/PANGAEA.863919.

Chevalier, M., 2018, GBIF database for CREST: , p. https://figshare.com/s/cf9fd5074af921d17c2b, doi:10.6084/m9.figshare.6743207.

Chevalier, M., and Chase, B.M., 2015, Southeast African records reveal a coherent shift from high- to low-latitude forcing mechanisms along the east African margin across last glacial–interglacial transition: Quaternary Science Reviews, v. 125, p. 117–130, doi:10.1016/j.quascirev.2015.07.009.

Chevalier, M., Chase, B.M., Quick, L.J., Dupont, L.M., and Johnson, T.C., 2020, Temperature change in subtropical southeastern Africa during the past 790,000 years:, doi:10.1594/PANGAEA.915923.

Chevalier, M., Cheddadi, R., and Chase, B.M., 2014, CREST (Climate REconstruction SofTware): a probability density function (PDF)-based quantitative climate reconstruction method: Climate of the Past, v. 10, p. 2081–2098, doi:10.5194/cp-10-2081-2014.

Dupont, L.M., Caley, T., and Castañeda, I.S., 2019, Effects of atmospheric CO2 variability of the past 800 kyr on the biomes of southeast Africa: Climate of the Past, v. 15, p. 1083–1097, doi:10.5194/cp-15-1083-2019.

Dupont, L.M., Caley, T., Kim, J.-H., Castañeda, I.S., Malaizé, B., and Giraudeau, J., 2011, Glacial-interglacial vegetation dynamics in South Eastern Africa coupled to sea surface temperature variations in the Western Indian Ocean: Climate of the Past, v. 7, p. 1209–1224, doi:10.5194/cp-7-1209-2011.

Fisher, R.A., Steven Corbet, A.., and Williams, C.B., 1943, The Relation Between the Number of Species and the Number of Individuals in a Random Sample of an Animal Population: British Ecological Sosciety, v. 12, p. 42–58.

GBIF.org, 2018a, Anthocerotopsida occurrence data downloaded on September 13th, 2018:, doi:10.15468/dl.czfuzq.

GBIF.org, 2018b, Cycadopsidae occurrence data downloaded on March 30th, 2018:, doi:10.15468/dl.lnzrov.

GBIF.org, 2018c, Gingkoopsidae occurrence data downloaded on March 30th, 2018:, doi:10.15468/dl.mvduln.

GBIF.org, 2018d, Gnetopsidae occurrence data downloaded on March 30th, 2018:, doi:10.15468/dl.prwbxf.

GBIF.org, 2018e, Liliopsida occurrence data downloaded on September 13th, 2018:, doi:10.15468/dl.h891rx.

GBIF.org, 2018f, Lycopodiopsida occurrence data downloaded on September 13th, 2018:, doi:10.15468/dl.7g3ylt.

GBIF.org, 2018g, Magnoliopsida occurrence data downloaded on March 30th, 2018:, doi:10.15468/dl.wamwmk.

GBIF.org, 2018h, Pinopsidae occurrence data downloaded on March 30th, 2018:, doi:10.15468/dl.rldwzj.

GBIF.org, 2018i, Polypodiopsida occurrence data downloaded on September 13th, 2018:, doi:10.15468/dl.lpx1qf.

Hill, M.O., 1973, Diversity and Evenness: A Unifying Notation and Its Consequences: Ecology, v. 54, p. 427–432, doi:10.2307/1934352.

Johnson, T.C. et al., 2016, A progressively wetter climate in southern East Africa over the past 1.3 million years: Nature, v. 537, p. 220–224, doi:10.1038/nature19065.

Jouzel, J. et al., 2007, Orbital and millennial Antarctic climate variability over the past 800,000 years.: Science, v. 317, p. 793–796, doi:10.1126/science.1141038.

Jouzel, J., and Masson-Delmotte, V., 2007, EPICA Dome C Ice Core 800KYr deuterium data and temperature estimates:, doi:10.1594/PANGAEA.683655.

Laskar, J., Robutel, P., Joutel, F., Gastineau, M., Correia, A.C.M., and Levrard, B., 2004, A long-term numerical solution for the insolation quantities of the Earth: Astronomy and Astrophysics, v. 428, p. 261–285, doi:10.1051/0004-6361:20041335.

Legendre, P., and Legendre, L.F.J., 2012, Numerical ecology: Elsevier, v. 24.

Lisiecki, L.E., and Raymo, M.E., 2005a, (Appendix 1) Global Plio-Pleistocene stack of benthic oxygen isotope records, *in* PANGAEA, doi:10.1594/PANGAEA.701576.

Lisiecki, L.E., and Raymo, M.E., 2005b, A Pliocene-Pleistocene stack of 57 globally distributed benthic δ 18 O records: Paleoceanography, v. 20, p. PA1003, doi:10.1029/2004PA001071.

Margalef, D.R., 1957, Information theory in ecology: Memorias de la Real Academica de ciencias y artes de Barcelona, v. 32, p. 374–559, https://ci.nii.ac.jp/naid/10011534559/en/.

Pielou, E.C., 1966, The measurement of diversity in different types of biological collections: Journal of Theoretical Biology, v. 13, p. 131–144, doi:10.1016/0022-5193(66)90013-0.

R Core Team, 2018, R: A Language and Environment for Statistical Computing:, http://www.r-project.org/.

Rehfeld, K., Marwan, N., Heitzig, J., and Kurths, J., 2011, Comparison of correlation analysis techniques for irregularly sampled time series: Nonlinear Processes in Geophysics, v. 18, p. 389–404, doi:10.5194/npg-18-389-2011.